

39

AT-Rapport

ROYAUME DE BELGIQUE

MINISTÈRE DES AFFAIRES ÉCONOMIQUES
ADMINISTRATION DES MINES – SERVICE GÉOLOGIQUE DE BELGIQUE

13, rue Jenner – 1040 Bruxelles

Bed features in the estuary of the Schelde (Belgium)

by

S. WARTEL

PROFESSIONAL PAPER 1974 N° 11

P

ROYAUME DE BELGIQUE

MINISTÈRE DES AFFAIRES ÉCONOMIQUES
ADMINISTRATION DES MINES – SERVICE GÉOLOGIQUE DE BELGIQUE

13, rue Jenner – 1040 Bruxelles

Bed features in the estuary of the Schelde (Belgium)

by

S. WARTEL

PROFESSIONAL PAPER 1974 N° 11

BED FEATURES IN THE ESTUARY OF THE SCHELDE (BELGIUM).

by S. WARTEL

ABSTRACT.

Bed features in a section of the estuary of the Schelde, located between the confluence of the Schelde and the Rupel and the Belgian-Dutch frontier, are studied with an echosounder. Large scale ripples, with heights between 0.3 m and 3 m occur. The ratio, ripple height : mean grain size diameter, varies between 1.5×10^3 and 3×10^4 . Mud layers occur downstream. Some irregular features (pits and humps) are due to human influence. The slopes of artificial dumped clay varies between 0,14 and 0,20, in agreement with underwater slopes in the Veerse Meer and the Oosterschelde (The Netherlands). All observations point to a decreasing stream power from the Schelde-Rupel confluence to the neighbourhood of Lillo.

KORTE INHOUD.

Bodemverschijnselen in het gedeelte van het estuarium van de Schelde, gelegen tussen de samenvloeiing van de Schelde en de Rupel en de Belgisch-Nederlandse grens, zijn bestudeerd met het echolood. Megarippels met een hoogte van 0.3 m tot 3 m komen voor. De verhouding, rippelhoogte tot gemiddelde korrelgrootte bedraagt : $1,5 \times 10^3$ tot 3×10^4 . Sliblagen worden in het stroomafwaartse gedeelte aangetroffen. Sommige onregelmatigheden zijn te wijten aan menselijk ingrijpen. De onderwaterhelling van kunstmatig afgezette klei bedraagt 0,14 à 0,20 in overeenstemming met natuurlijke

onderwaterhellingen in het Veerse Meer en de Oosterschelde (Nederland). Alle waarnemingen wijzen op een dalende stroomkompetentie van de samenvloeiing Schelde-Rupel naar Lillo toe.

RESUME

Le fond de l'estuaire de l'Escaut, entre le confluent Escaut-Rupel et la frontière belgo-hollandaise, est étudié à l'aide d'un écho-sondeur. La configuration montre des mégarides entre 0.3 m et 3 m de Haut. La relation entre la hauteur des rides et le diamètre moyen du sédiment varie entre 1.5×10^3 et 3×10^4 . Des couches de vases occupent les parties en aval. Quelques irrégularités du fond (creux et bosses) sont dues essentiellement à l'intervention humaine (dragages). La pente des dépôts artificiels de vase a des valeurs 0,14 à 0,20 semblables à des pentes naturelles sous-aquatiques dans le Veerse Meer et l'Oosterschelde (Pays-Bas). Toutes les observations indiquent une décroissance de la compétence du courant du confluent Escaut-Rupel jusqu'aux environs de Lillo.

1. INTRODUCTION

Knowledge of the bottom configuration of an estuary is important for a better understanding of the problems concerned with sedimentary dynamics. The echosounder has already proved to be a practical instrument for this kind of research; moreover not only the bottom configuration, but also some indications concerning the bottom composition are recorded.

In order to contribute to the knowledge of the bottom configuration in the estuary of the Schelde a large number of echosounding profiles, parallel to the axis of the main channel, were recorded between the Schelde-Rupel confluence (Rupelmouth) and the Belgian-Dutch frontier (fig. 1). Some areas, studied more in detail, are discussed here. The choice of the areas was suggested by earlier studies (BASTIN, A., 1973; WARTEL, S., 1972). All the measurements were made between July 1972 and March 1973.

2. METHODS.

The echosoundings were recorded with a KELVIN HUGHES echosounder (35 Kc/sec), expected for the profiles 28 (fig. 11) and 31 (fig. 9) where an ATLAS echosounder (30 Kc/sec) was used. Positions were determined with an error less than 5 m, every 100 m or less by means of sextants and river maps on scale 1 : 5.000 (ANTWERPSE ZEEDIENSTEN, 1972), thus giving the length of bottom structures with an accuracy of at least 10 %. The absolute depth for a given place was recorded with an error estimated less than 1 % and the height of the bottom structures could thus be calculated with the same accuracy.

3. DISCUSSION.

a) Major sediment accumulations.

A longitudinal profile along the main channel and covering the whole section shows a succession of sediment accumulations (bars) which form shallower parts, oriented obliquely to the channel, on the river bed. The distance between the top of two successive bars is 2 to 3 km, while the difference in height between the top of a bar and the lowest point of the succeeding depression may be 5 to 10 m.

Profile 20, fig. 10, shows the bar at Fort De Parel with a difference in height of 8 m. The slope S of these macro-structures, measured along the axis of the main channel is :

$$S = \operatorname{tg} \alpha = 0,004 \text{ to } 0,007 \quad (\alpha \text{ very small})$$

(where α is the angle with the horizontal).

b) Large - scale ripples.

The most prominent regular structures observed are the large - scale ripples (ALLEN, J.R.L., 1968). They occur anywhere where the bottom sediment consists of well sorted sand (fig. 3A). The smallest ripples detected with the echosounder are approximately 0.3 m in height and several meters in length (profiles 2 to 5, fig. 14), while the largest are 3 m or more in height and 100 m or more in length (profile 16, fig. 6). The relationship between the mean grain size diameter D and the ripple height H at a given place is found to be :

place	D	H	
M 9	0,14 mm	3000 mm	$H = 2,2 \times 10^4 D$
M 11	0,1 mm	3000 mm	$H = 3 \times 10^4 D$
M 1	0,12 mm	300 mm	$H = 2,5 \times 10^3 D$
M 2	0,2 mm	300 mm	$H = 1,5 \times 10^3 D$

These values are within the limits accepted for large scale ripples by ALLEN, J.R.L., 1968 :

$$H = 2 \times 10^2 D \text{ to } 1 \times 10^5 D.$$

The largest ripple heights occur upstream of Burcht, while diminishing ripple heights are observed in a downstream direction from Burcht to Oosterweel (fig. 4).

The ratio L/H, ripple length over height, is rather constant and varies between 20 and 60. Variation in length and height are to be explained by a number of factors.

GUY, H.P. et al. (1966) have shown that a decrease in boundary shear produces a decrease in ripple dimensions, the ratio L/H being constant. In the estuary of the Schelde the highest values for the shear velocity (and thus also the boundary shear stress) were measured in the section upstream of Burcht, while the lowest values occur between Oosterweel and Lillo (WARTEL, S., 1973). Another factor is the relationship between ripple height and grain size (SIMONS, D.B. et al., 1965) according to which smaller grain sizes give smaller ripple dimensions. Several cumulative grain size distributions for sediments located at different places between the Rupelmouth and the Belgian-Dutch frontier are given in fig. 3A, 3B and 3C. As the analyzed samples were not collected simultaneously of echosounding nor at exactly the same places of the echosounding profiles, a rigorous comparison will not be possible. Nevertheless, as only major trends in sediment distribution are considered here, there are no reasons to believe that important changes in sediment distributions occurred between sampling and echosounding.

The coarsest sediments occur upstream of Burcht and range from gravels (at approximately 2 km downstream the Rupelmouth, WARTEL, S., 1972) to strong bimodal coarse and medium sand (M8, fig. 2A and 3A) and medium sand (M9, fig. 2A and 3A) at 5 km downstream the Rupelmouth and still finer medium sand (M11, fig. 2B and 3A) near Antwerpen. Between Antwerpen and the Belgian-Dutch frontier finer sediments, containing large amounts of particles finer than 62μ (silt and clay) (B1 and B2, fig. 2B, 2C and 3B) and mud (represented by samples B26, B28, B29, fig. 2D and 3C) occur. Downstream of Lillo the sand deposits become coarser again (e.g. samples A and B20, fig. 2D and 3B). Thus a rough relationship between grainsize and ripple dimensions exists.

From the foregoing one may accept that both a decrease of boundary shear stress and a decrease in grain size are accompanied by a decrease of ripple dimensions from the Rupelmouth to Lillo. The increase in grain size of the sand deposits downstream of Lillo is also recognizable in a small increase in ripple dimensions as shown in fig. 4 (triangles).

Another phenomenon is shown in fig. 12, profiles 6 and 7 measured across the bar at Belgische Sluis (fig. 2C). Here the ripples occurring at the foot of the bar (n° 4 to 6, profile 6 and 9 to 13, profile 7) disappear to the top of the bar, which is rather smooth. At the moment of measurement a strong landward current prevailed. Thus one may suppose that this transition from a rippled to a smooth surface is due to a local increase in boundary shear stress caused by the smaller depth at the top of the bar.

A bottom configuration showing large scale ripples corresponds to the "Lower flow regime" of SIMONS, D.B. et al., (1965). The influence of the ripple height on roughness is more important here than the influence of sediment particles, which is an important criterion when sediment erosion has to be considered.

The stream power $\bar{u}\tau$ (fig. 5) where \bar{u} represents the average velocity and τ the boundary shear stress (SIMONS, D.B. & RICHARDSON, E.V., 1966) varies between 1,06 and 1,97 g/sec.cm. (for sediments with median diameter between 0,1 and 0,3 mm). On the top of a bar the stream power locally increases and the river evolves into a higher flow regime (transitional flow) as has been shown for the bar at Belgische Sluis.

c) Irregularities.

At some places the bottom configuration shows irregularities such as scour pits and mounds with heights of a few meters and some ten meters in length. In most cases they are due to human influence (e.g. construction of the E-3 tunnel, profile 14, fig. 7 or dredging works, profile 8 and 9, fig. 12, etc ...). The mounds of profile 15 (fig. 6) are remarkable as they were artificially built by dumping of clay (Rupelian) originated from the trench of the E-3 tunnel works. This clay shows stable underwater slopes :

$$S = \operatorname{tg} \alpha = 0,1435 \text{ to } 0,2000 \quad (\alpha = 7,6^\circ \text{ to } 11,3^\circ)$$

Recent investigations by scuba diving (FAAS, R. & WARTEL, S., 1973, paper in preparation) show these slope-values to be common for the débris slopes at the foot of underwater cliffs in the Eastern Schelde and sections of the Veerse Meer (The Netherlands).

d) Clay and mud deposits.

In addition to variations in bottom structures, differences in the strenght of the recorder acoustic reflection reveal some indication concerning the bottom composition (LEENHARDT, O., 1969; LI, W.N. & TAYLOR SMITH, D., 1969).

Profiles 20, 21 and 22 (fig. 10 and 11), measured across the bar at Fort De Parel, show a completely smooth bottom (some irregularities are due to dredging of the channel). The recorded echo is rather strong, which is characterized by a broad heavy recording. Sampling in this environment shows the presence of a very poorly sorted sand-silt-clay (SHEPARD, F.P., 1954). The absence of ripples here agrees with the sediment type present. The strong echo can be explained by an increase in interparticle attraction, due to the poorly sorting of the sediment and the high clay content, whereby the attenuation coefficient of the sound in the bottom sediment is strongly reduced (LI, W.N. & TAYLOR SMITH, D., 1969).

At other places a double echo was recorded when a mud layer (grain size compositions as in fig. 3C), with low density and a certain minimum thickness lies on a more dense sandy surface. A first echo is generated when the density of the mud reaches 1.05 (OWAKI, N., 1963). Part of the sound penetrates deeper into this fluid mud (MIGNIOT, C., 1968) and gives a second echo corresponding to the denser subsurface. Since the echo produces a rather broad band, corresponding to a depth of 0,2 m for the recorder used, on the recording paper, the thickness of the fluid mud layer must exceed 0,2 m before producing a recording of a separated double echo. Otherwise both echo recordings will melt together, and the presence of the fluid mud is no longer detectable in this way.

Several fluid mud deposits are present. Profile 21 (fig. 10) shows a depression filled with a fluid mud layer of 0.6 m thick and, at the left, a smaller depression with a fluid mud deposit 0,3 m thick. A depression, 800 m long and filled with a 4 m thick fluid mud layer, is shown in profile 28 (fig. 11). The mud layer can be followed outside the depression. A 0.6 m thick fluid mud layer also occurs in profile 9 (fig. 12).

All these fluid mud deposits occur between Ford De Parel and Belgische Sluis. In the upstream direction sandy mud and clay occur but no fluid mud.

From these observations it is clear that the sediments described as "mud" by BASTIN, A., (1973) have a much broader sense than the fluid mud deposits described by MIGNIOT, C. and others, and discussed in the foregoing paragraphs. The "mud" on the maps of BASTIN, A., must be considered to a larger extent as being clayey sand, which react in an entirely different way on erosion forces.

The fluid mud deposits on the contrary occur in a more limited manner, not only by surface but also in thickness. Only in a few exceptional places (profile 28 fig. 11) entrance gully to the sluices of Zandvliet, Boudewijn and Kruisschans sluices and the former E3-tunnel dock (PETERS, J.J. & WOLLAST, R., 1969, and WARTEL, S., 1972), the thickness is larger than 2 to 3 m, while in most cases it is smaller than 0.3 to 0.5 m. It is interesting to compare with analogous fluid mud layers, recorded in the same way in the estuary of the Gironde (France), where fluid mud layers, several meters thick sometimes superimposed but clearly distinguishable from each other, occur (ALLEN, G.P. et al., 1970).

4. CONCLUSIONS

Echosounding records of bottom profiles parallel to the axis of the main channel of the Schelde between the Rupelmouth and the Belgian-Dutch frontier show remarkable differences in bottom configuration and composition.

The bottom varies from coarse sand, forming ripples with heights of several meters and occurring upstream of Burtch, to a finer sediment forming smaller ripples between Burtch and Antwerpen. The river in both areas is in the lower flow regime, with a stream power $\bar{U} \tau$ ranging from 1.06 to 1.97 g/sec.cm. Further downstream, the sediment becomes finer and more clay and mud occur. The surface becomes smoother as a consequence of the increasing clay content of the sediments and a decrease in stream power. From Fort De Parel until Belgische Sluis fluid mud deposits occur and grain size attains its minimum. Beyond this minimum grain size increases again in downstream direction while ripples are forming.

A general conclusion from these observations is that the area studied shows a zone of intense mud sedimentation (Fort De Parel - Belgische Sluis) and low stream power values ($\bar{U} \tau < 1.06$ g/sec.cm) located between two zones with coarser sediments and higher stream power.

5. AKNOWLEDGEMENTS.

The author thanks especially Ir. J. THEUNS, Director of the Hydrographic Survey of Antwerp (Ministry of Public Works), for the opportunity to perform this study and putting a ship and echosounder at his disposal.

6. BIBLIOGRAPHY.

- ALLEN, G.P., KLINGEBIEL, A. & de RESSEGUIER, A., 1970. Utilisation d'un echo-sondeur pour l'observation des faciès et des structures sédimentaires dans l'estuaire de la Gironde. (Bull. Inst. Géol. Bassin d'Aquitaine, 9, 193-200).
- ALLEN, J.R.L., 1968. Current ripples (North Holland publ. Comp., Amsterdam, 433 pp.).
- ANTWERPSE ZEEDIENSTEN, 1972. Peilkaarten van de Schelde op schaal 1 : 5.000. (Antwerpse Zeediensten, Ministerie van Openbare Werken, Antwerpen).
- BASTIN, A., 1973. Natural radioactive tracers and their use in Belgium. (Int. Atom. En. Ag., Techn. Rep., 145, 179-200).
- FAAS, R.W. & WARTEL, S., 1973. Study of bottom sediments and channel slopes in the Schelde-Estuary. (Kon. Belg. Inst. Nat. wet., prelim. rep., 32 pp.).
- GUY, H.P., SIMONS, D.B. & RICHARDSON, E.V., 1966. Summary of alluvial channel data from flume experiments. (I.S. Geol. Surv., Prof. Pap., 462-I, 96 pp.).
- LEENHARDT, O., 1969. Analyse en sondage sismique continu. (Rev. hydr. int., 46, 51-79).
- LI, W.N. & TAYLOR SMITH, D., 1969. Identification of sea-floor sediments using underway acoustics. (Geophys. prosp., 17, 231-247).
- MIGNIOT, C., 1968. Etude des propriétés physiques de différents sédiments très fins et de leur comportement sous des actions hydrodynamiques. (La Houille blanche, 23, 591-620).

- OWAKI, N., 1963. Note sur la détermination de la profondeur lorsque le fond est de vase molle. (Rev. hydr. int., 15, 43-46).
- PETERS, J.J. & WOLLAST, R., 1969. Envasement du chenal d'accès d'une écluse située sur un fleuve à marée. (La Houille blanche, 6, 623-630).
- SHEPARD, F.P., 1954. Nomenclature based on sand-silt-clay ratios. (Journ. Sed. Petr., 24, 151-158).
- SIMONS, D.B. & RICHARDSON, E.V., 1966. Resistance to flow in alluvial channels. (U.S. Geol. Surv., Prof. Pap., 422-J, 61 pp.).
- SIMONS, D.B., RICHARDSON, E.V. & NORDIN, C.F. Jr., 1965. Sedimentary structures generated by flow in alluvial channels. (Soc. Econ. Pal. Min., Spec. Publ., 2, 34-52).
- WARTEL, S., 1972. Sedimentologische opbouw van het Schelde estuarium. (Doktoraatsthesis, Univ. Leuven, 600 pp.).
- WARTEL, S., 1973. Shear velocity measurements and sediment transport in the Schelde estuary. (Bull. Soc. belg. Géol. - in press).

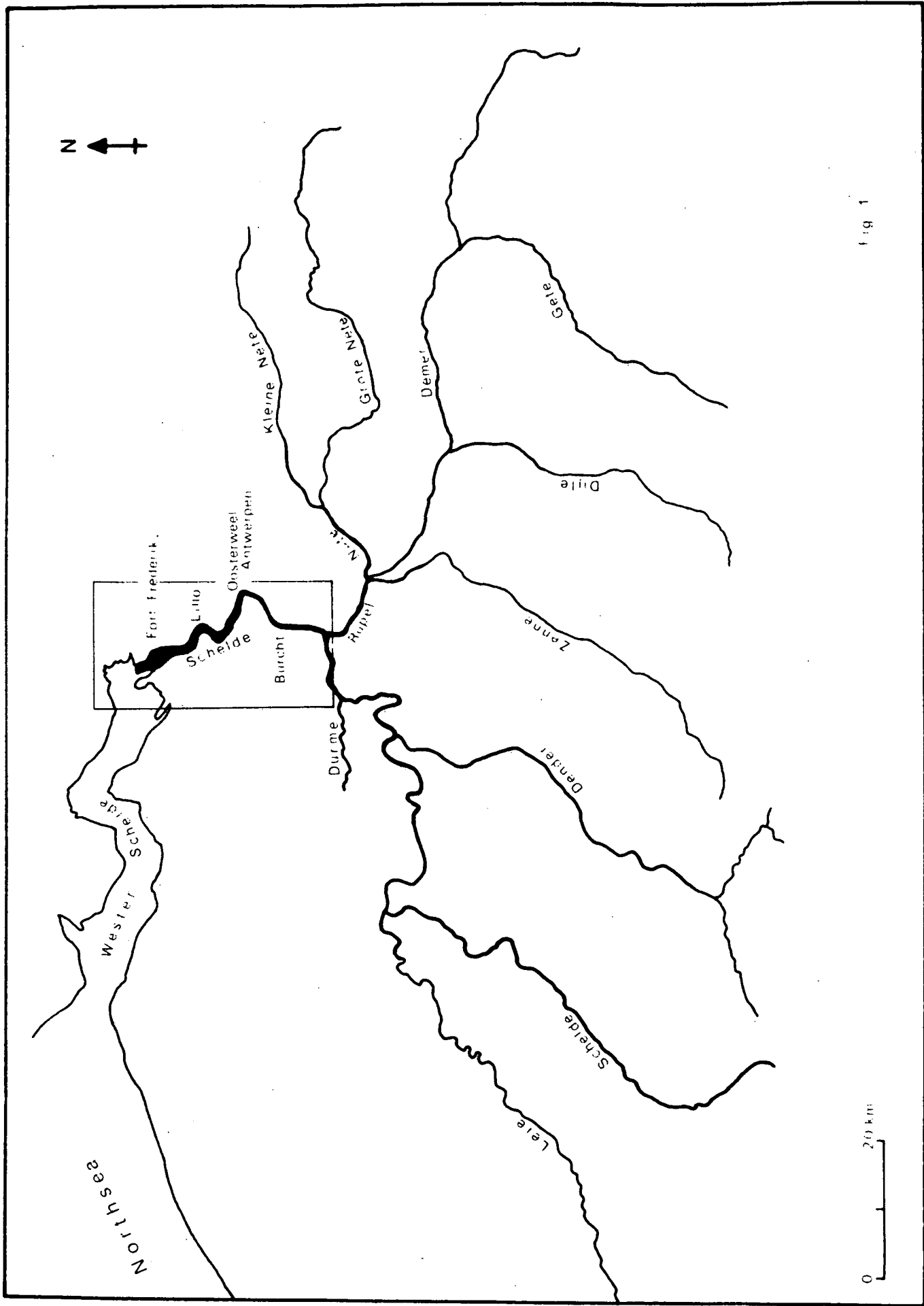


fig 1

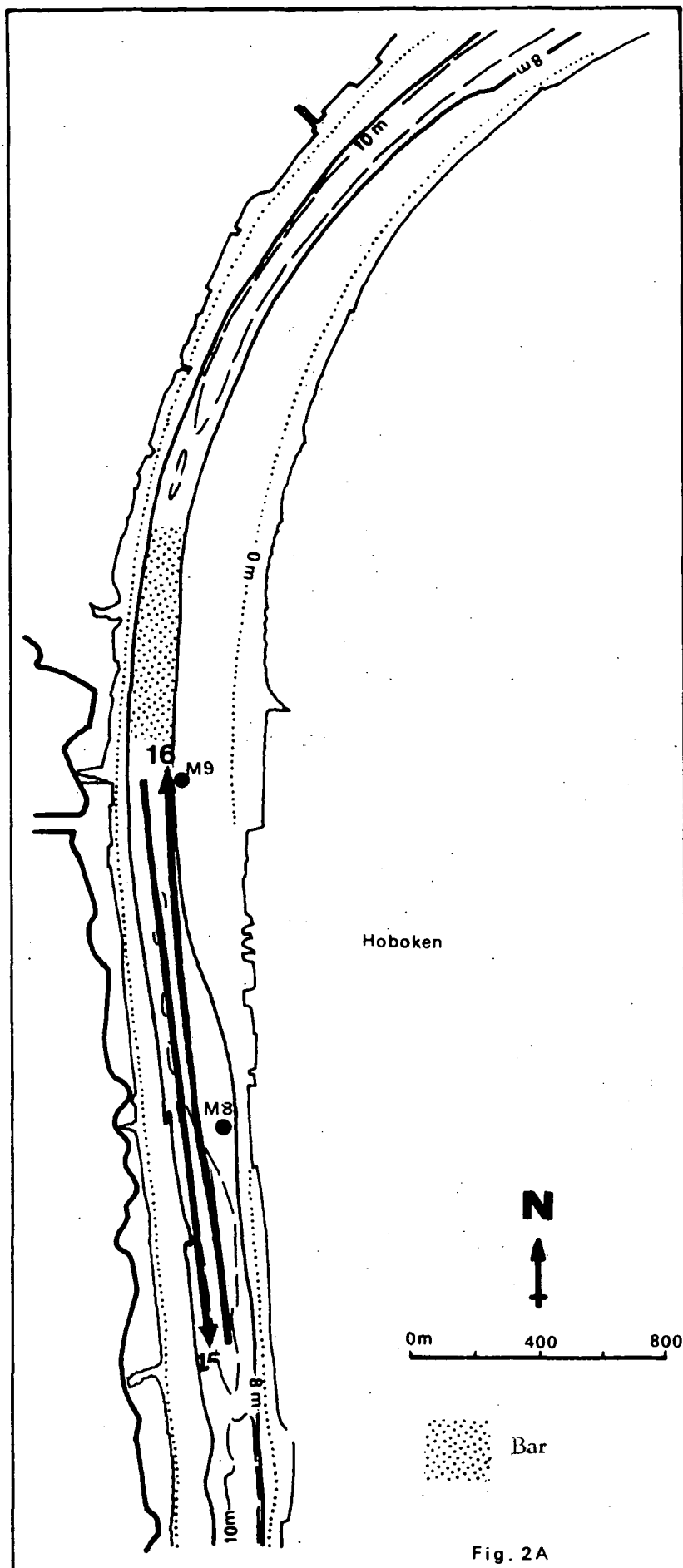


Fig. 2A

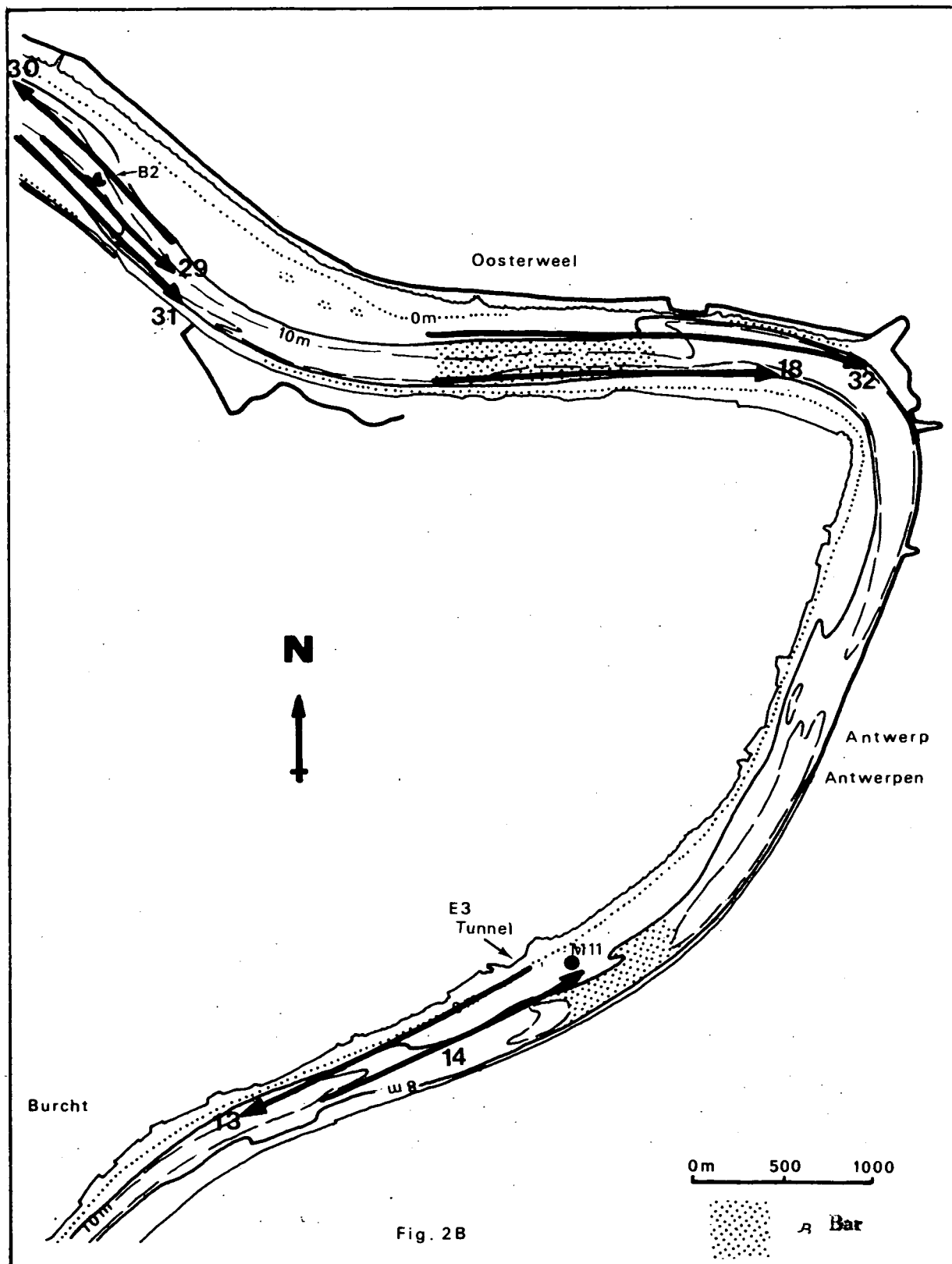


Fig. 28

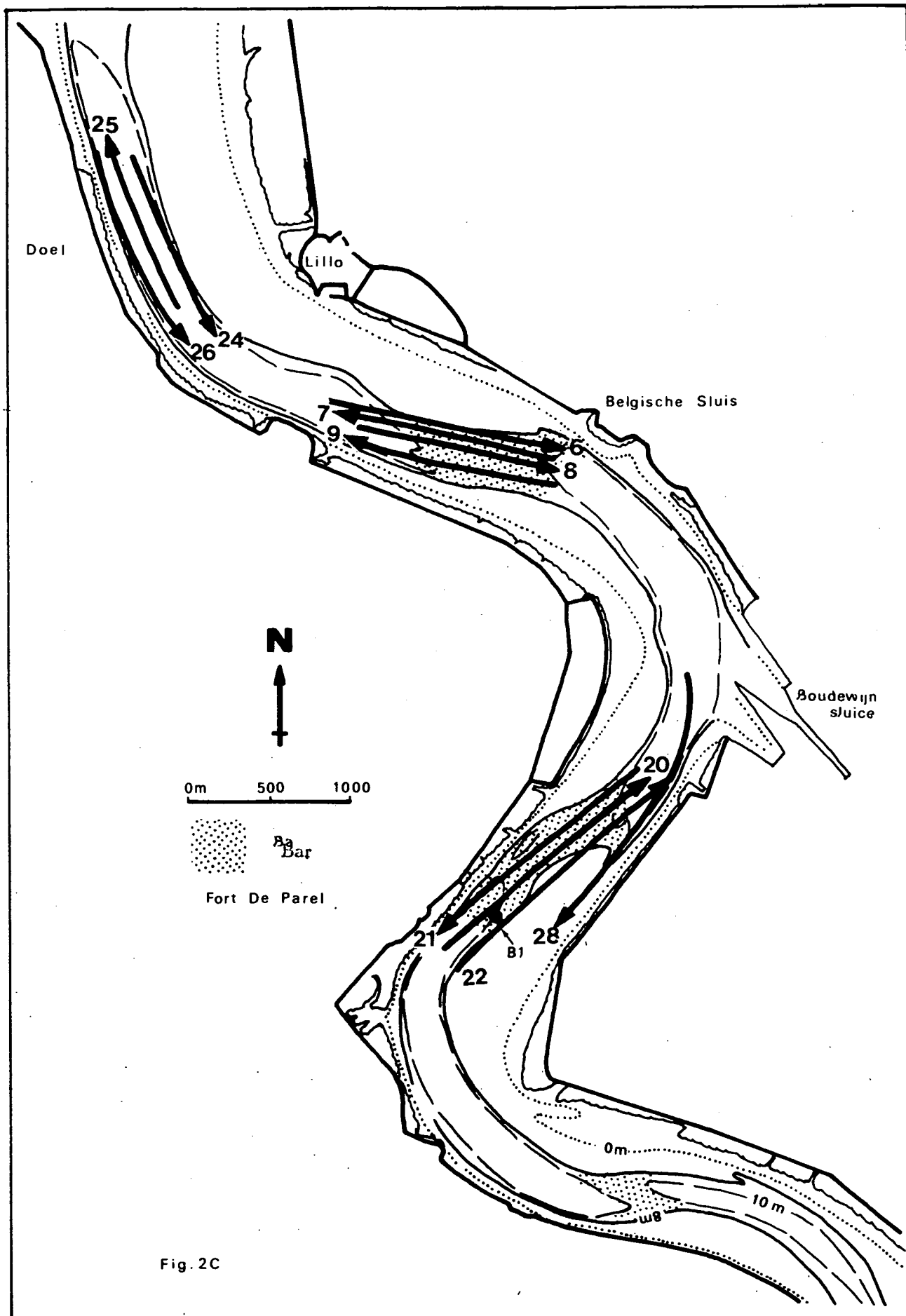


Fig. 2C

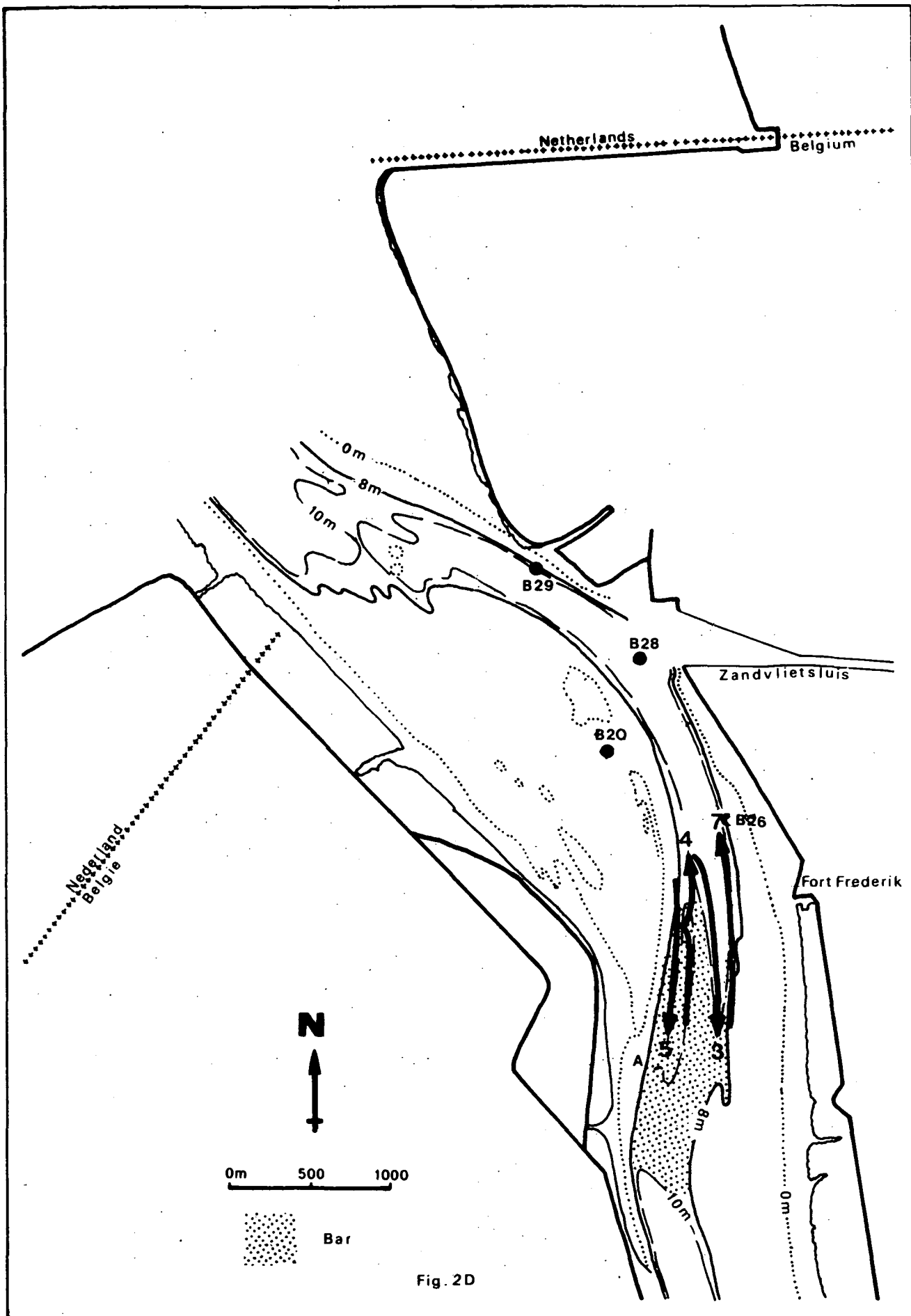


Fig. 2D

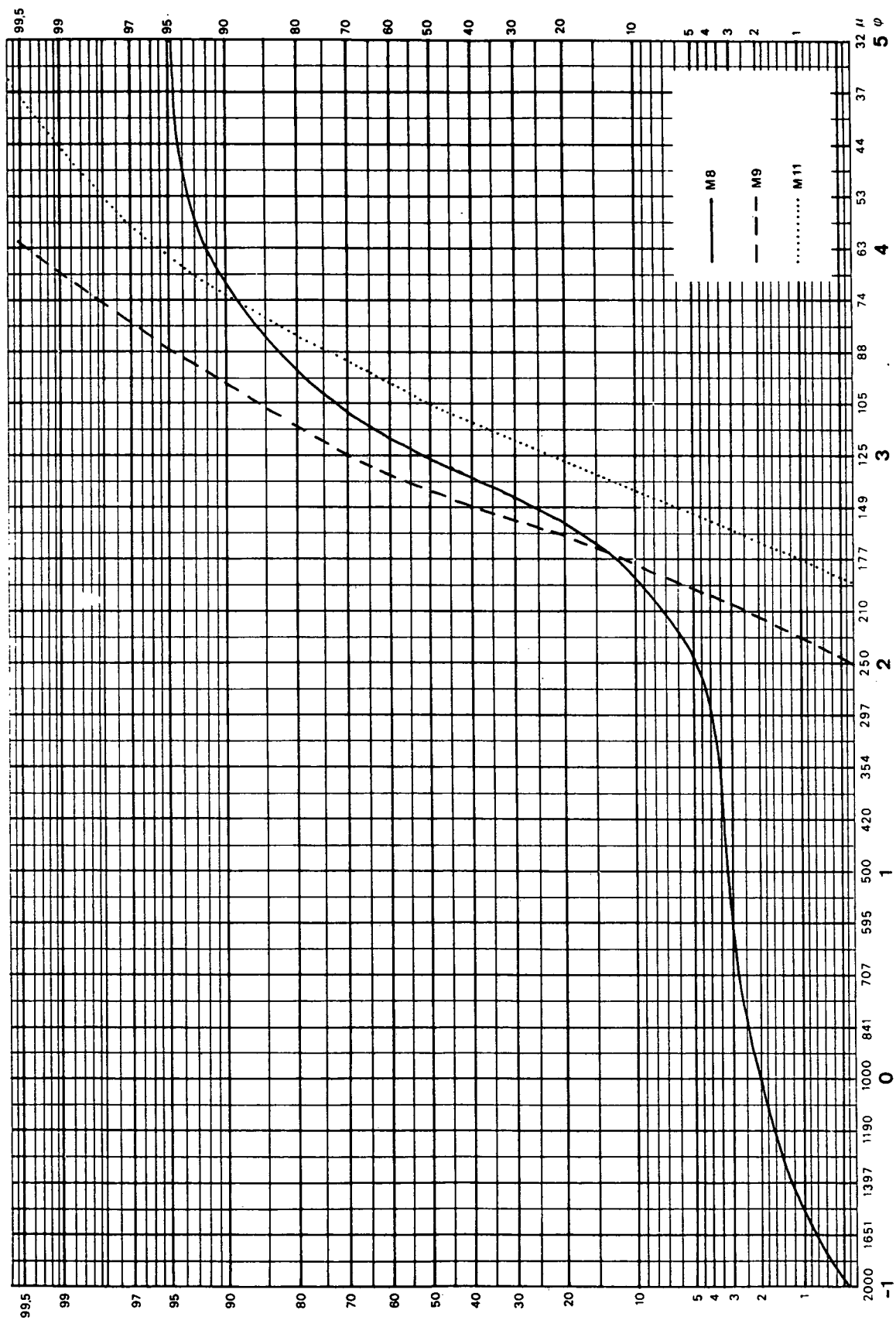


Fig. 3A Grain size analyses of bottom samples.

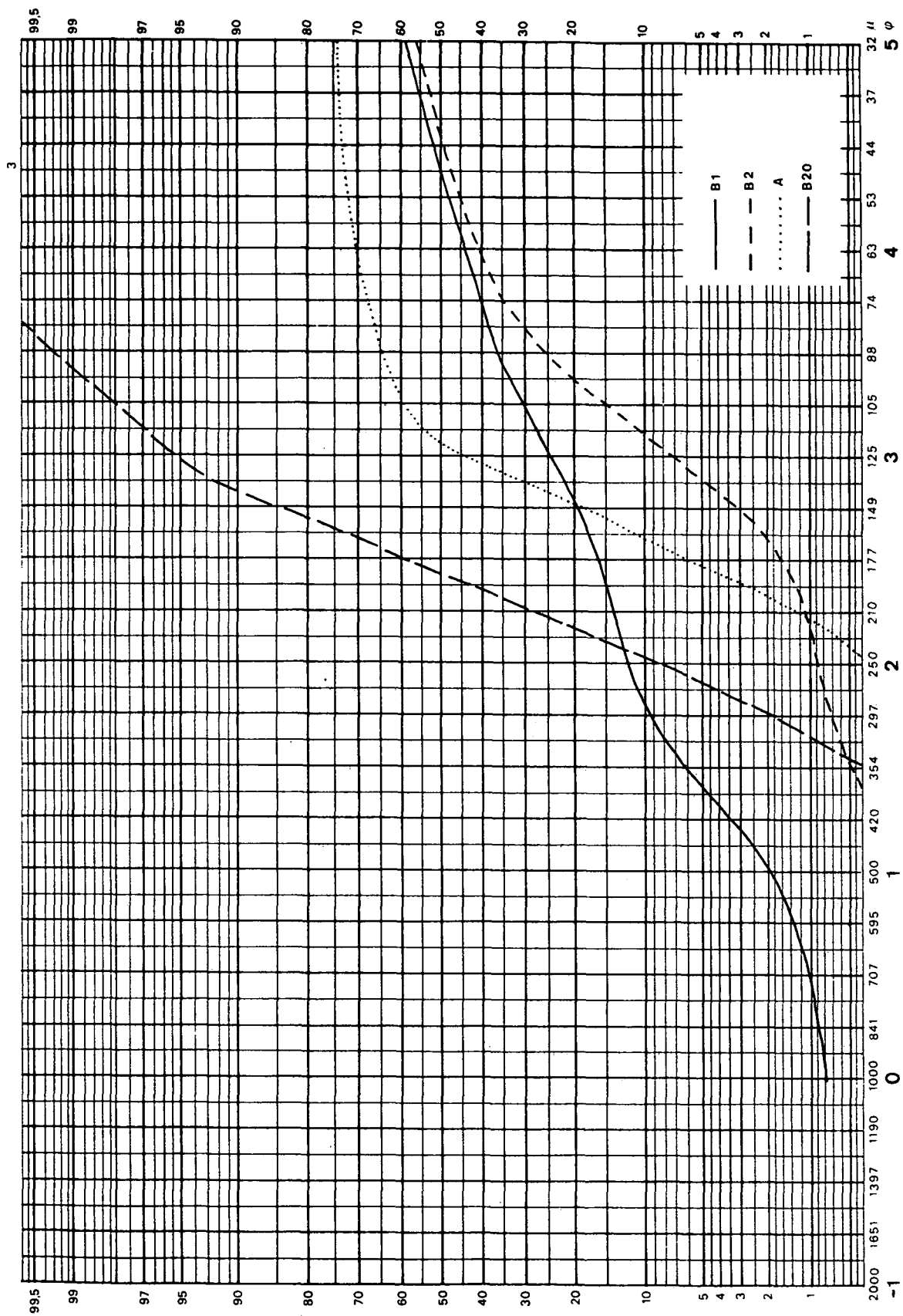


Fig. 3B Grain size analyses of bottom samples.

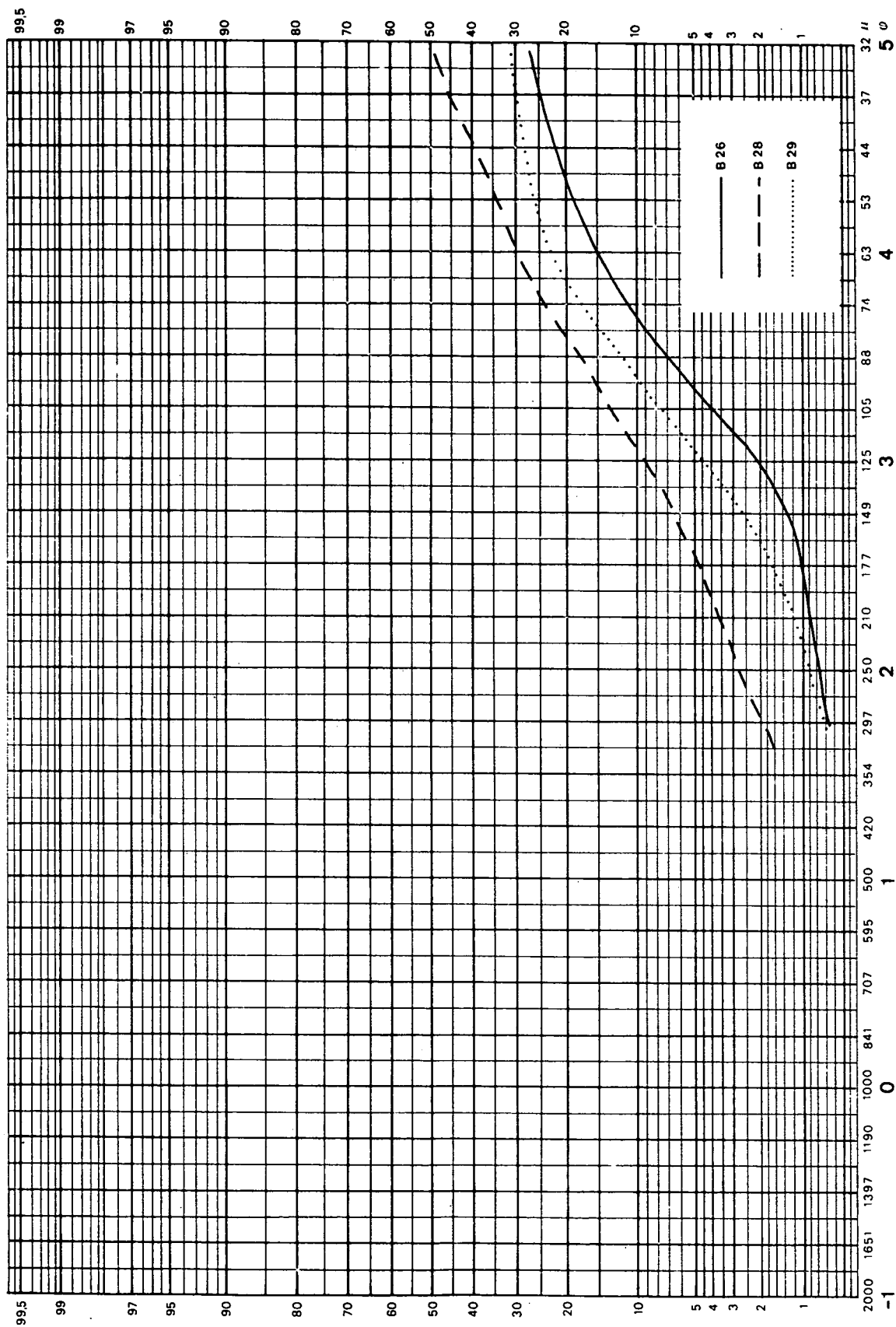


Fig. 3C Grain size analyses of bottom samples.

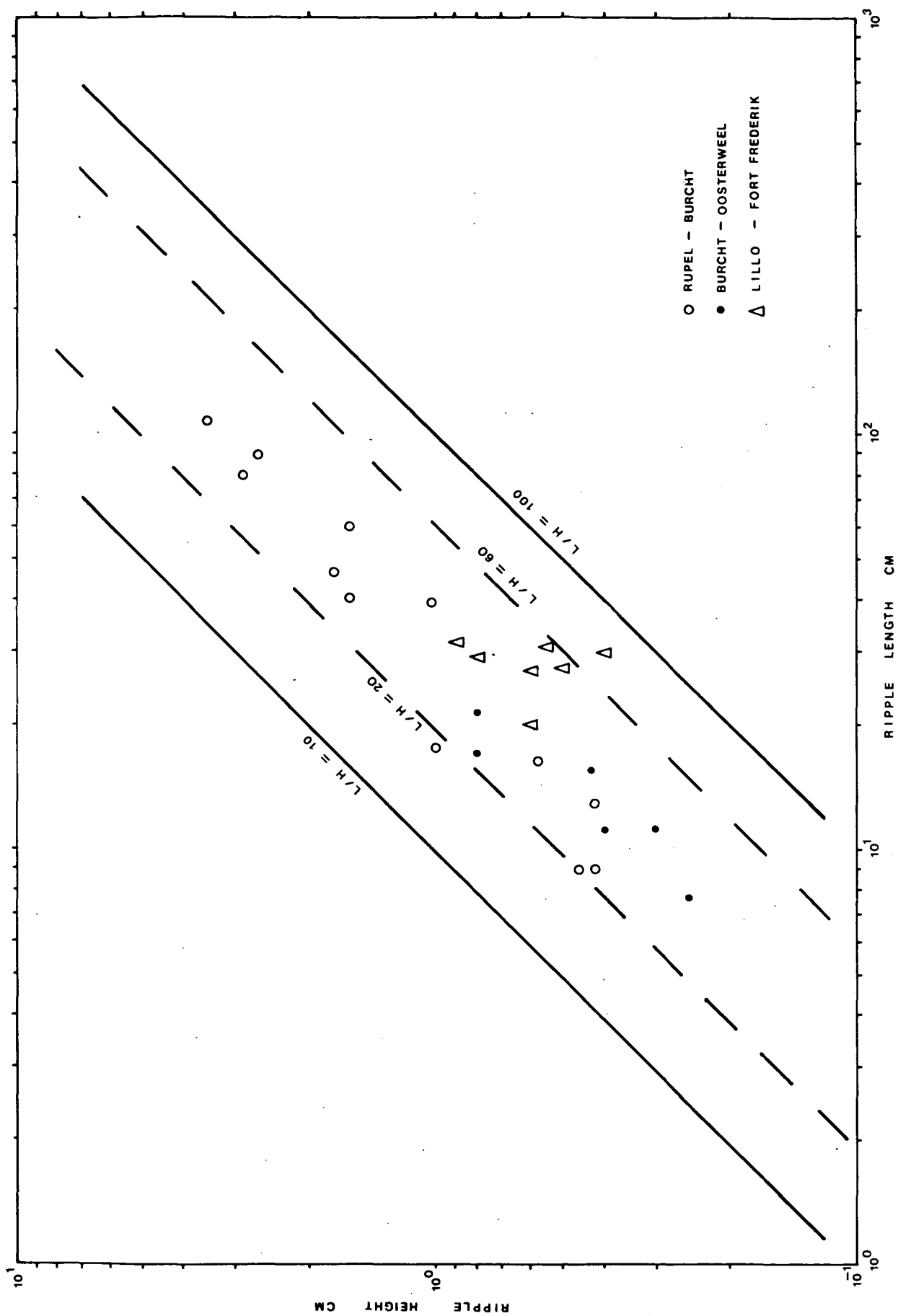


Fig. 4 Relationship between ripple dimensions.

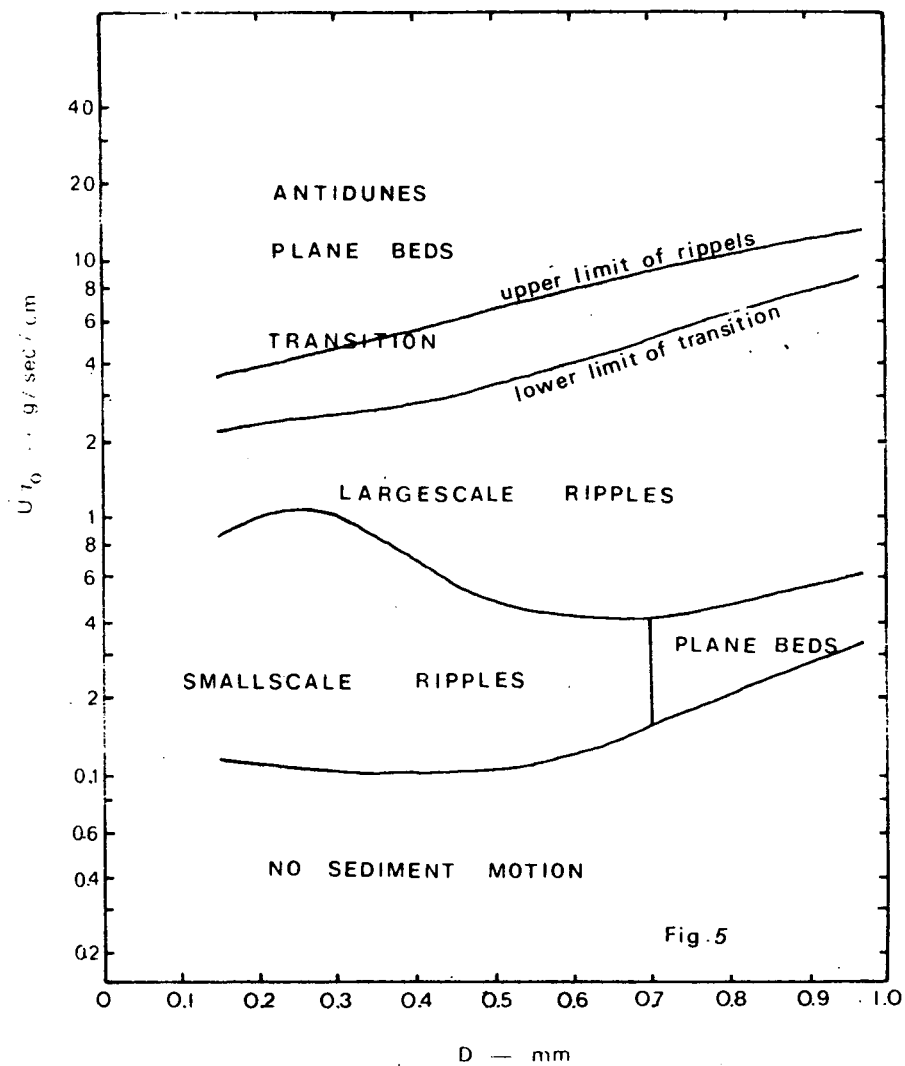


Fig. 6 Bottom profiles 15 and 16 - depths below water surface are given.

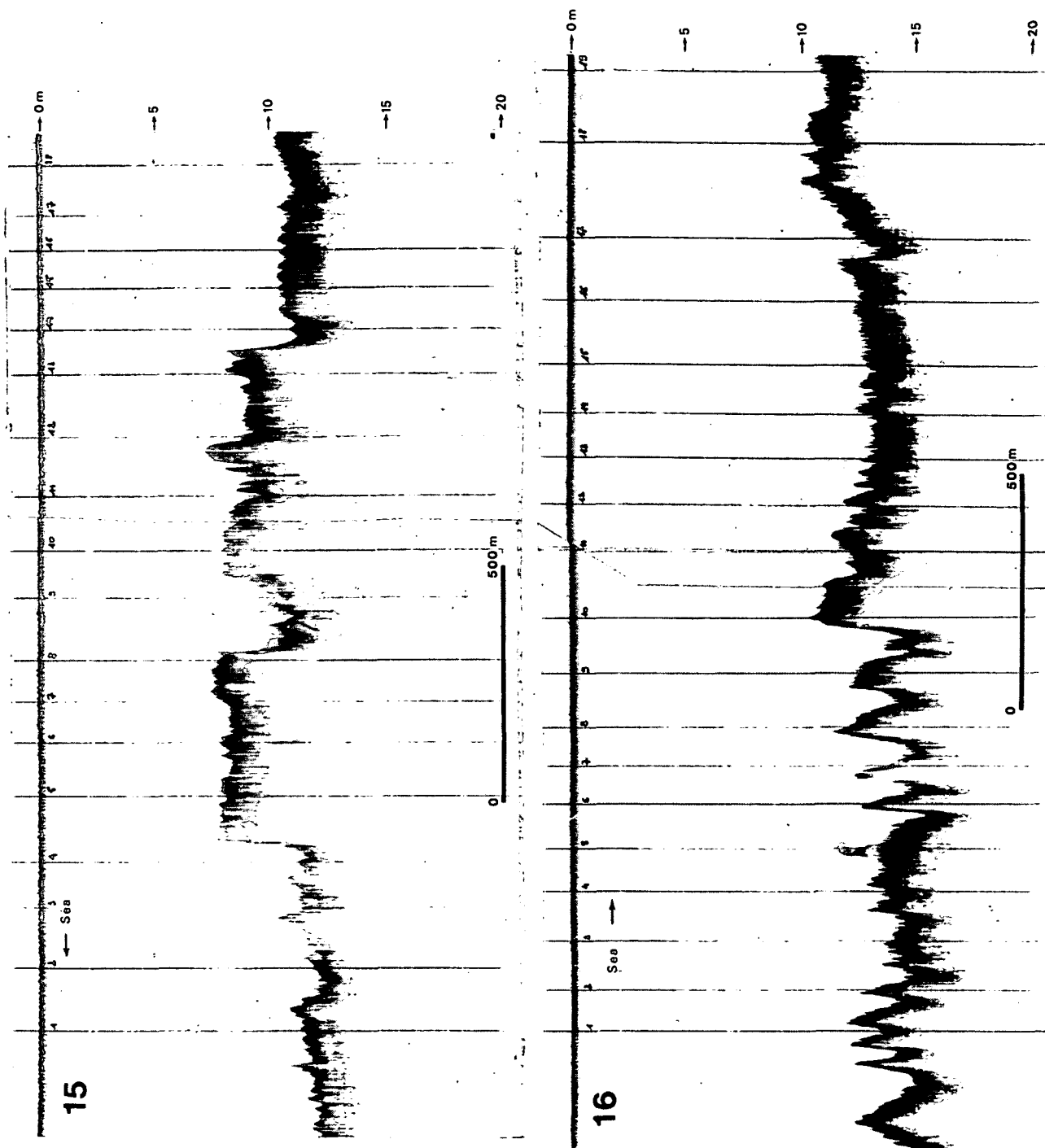


Fig. 7 Bottom profiles 13 and 14.

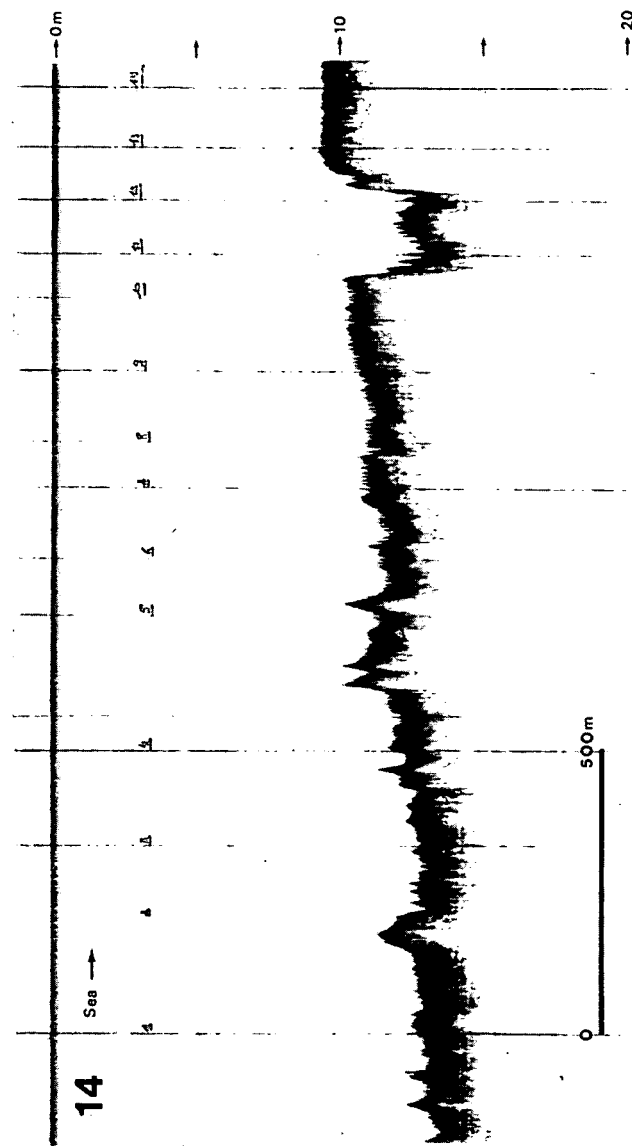
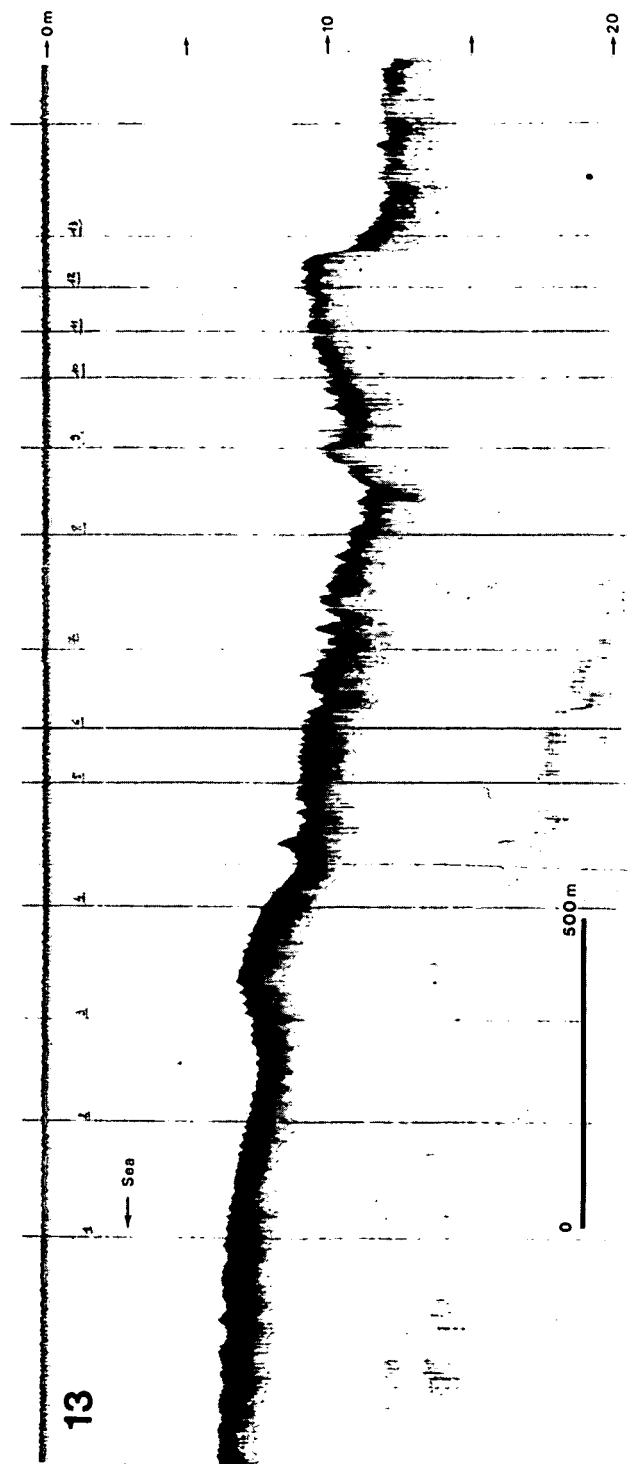
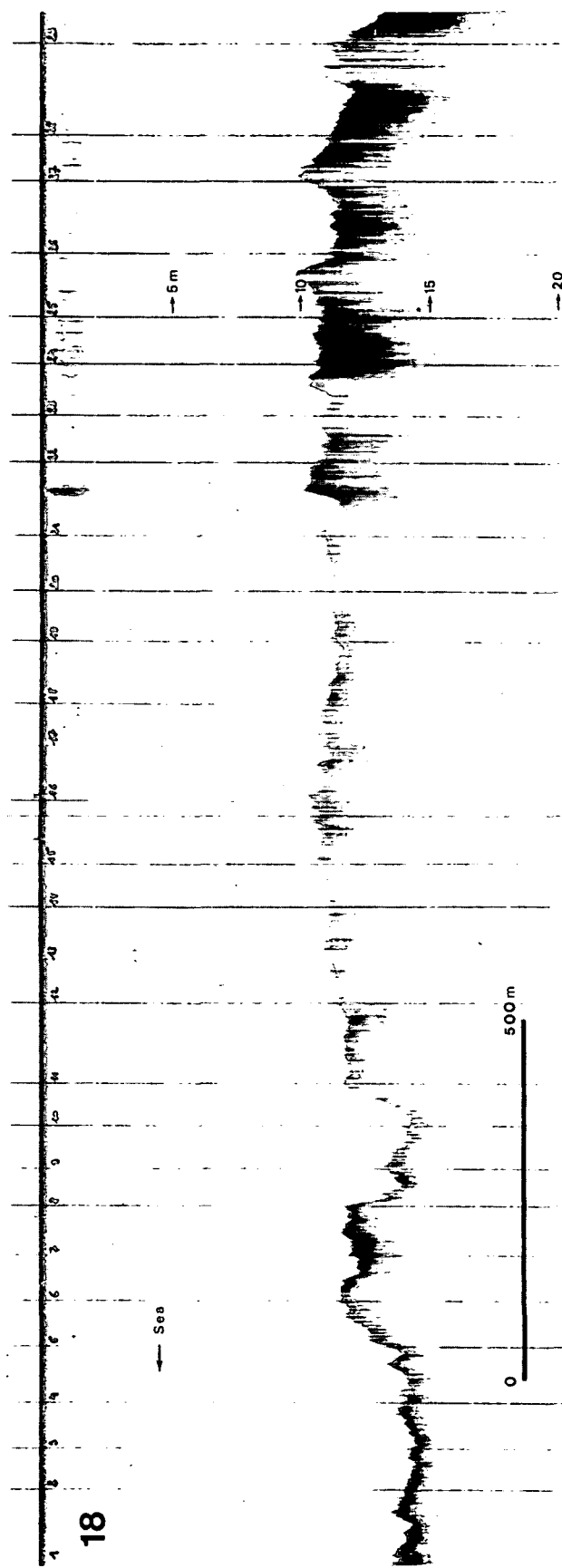
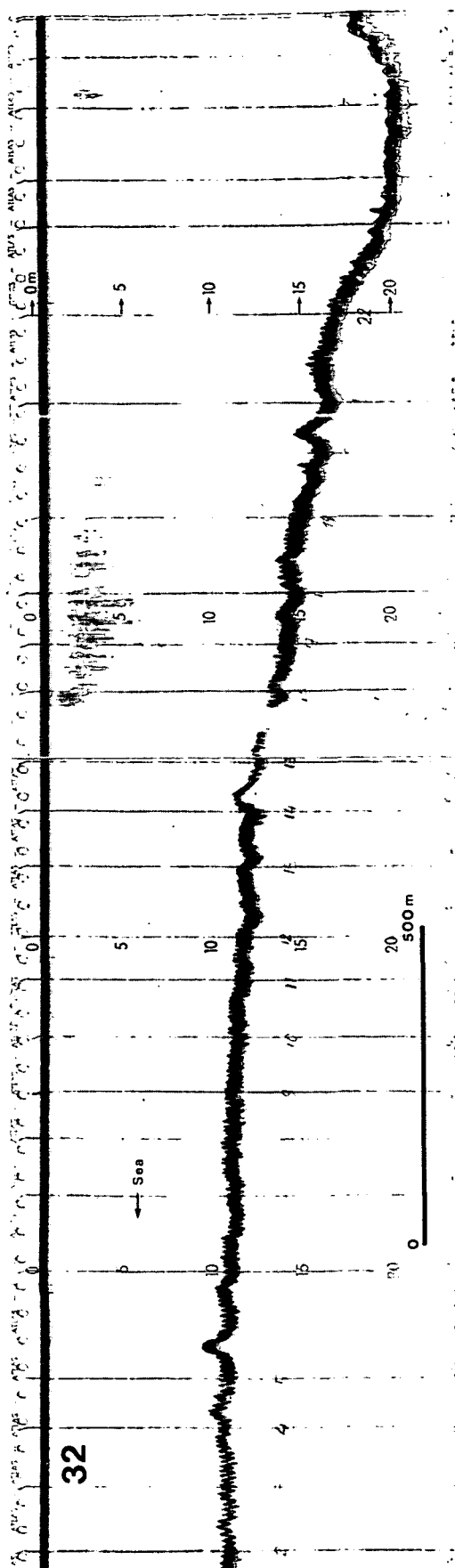


Fig. 8 Bottom profiles 18 and 32.



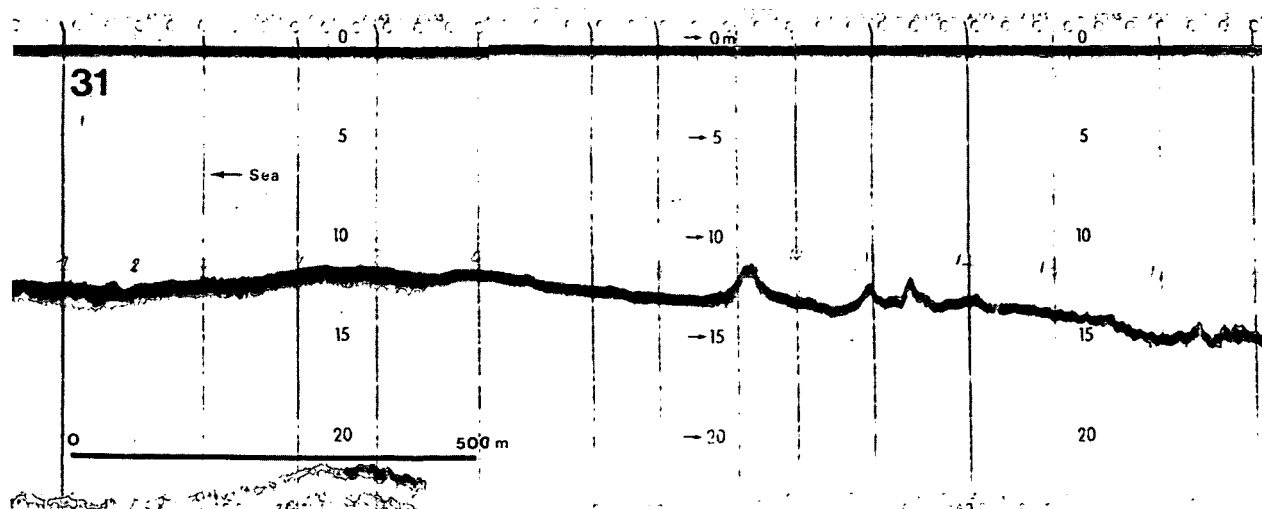
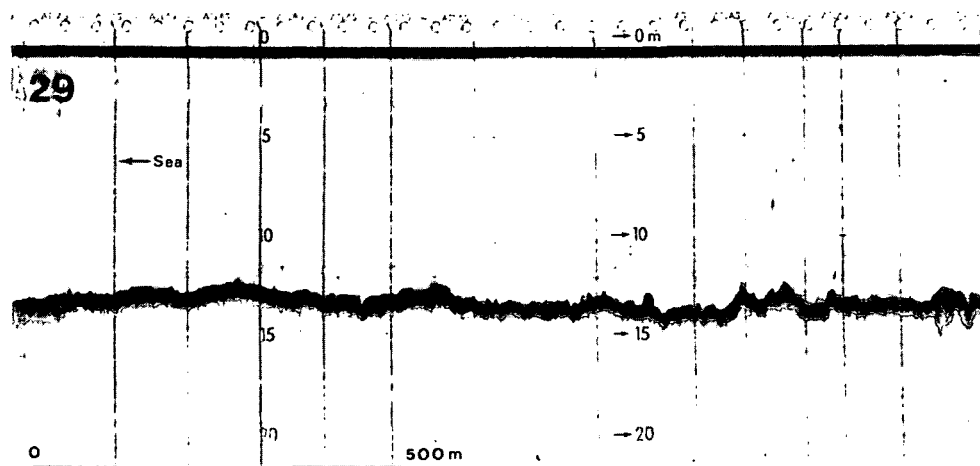
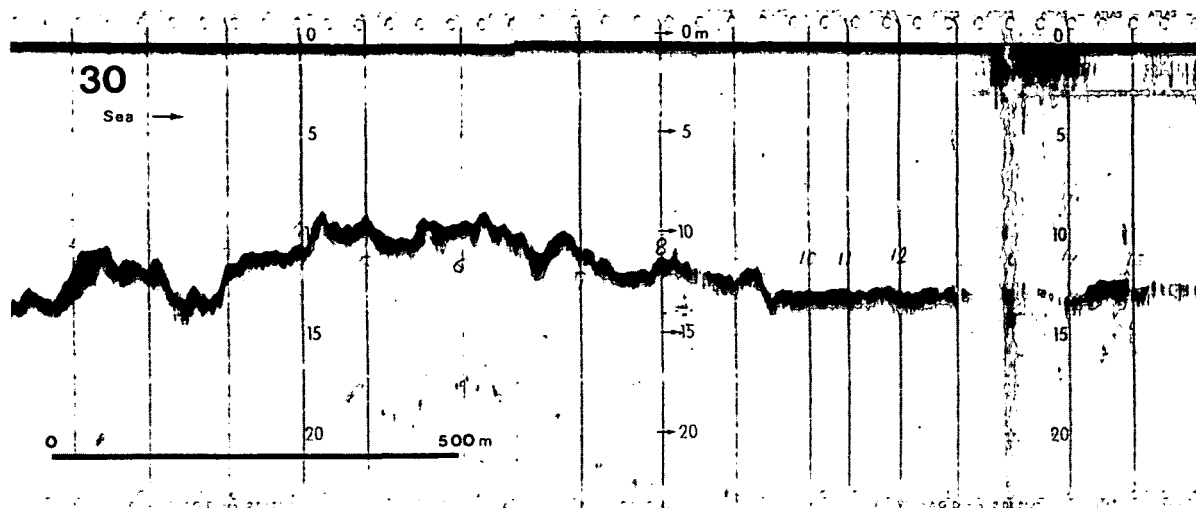


Fig. 9 Bottom profiles 29, 30 and 31.

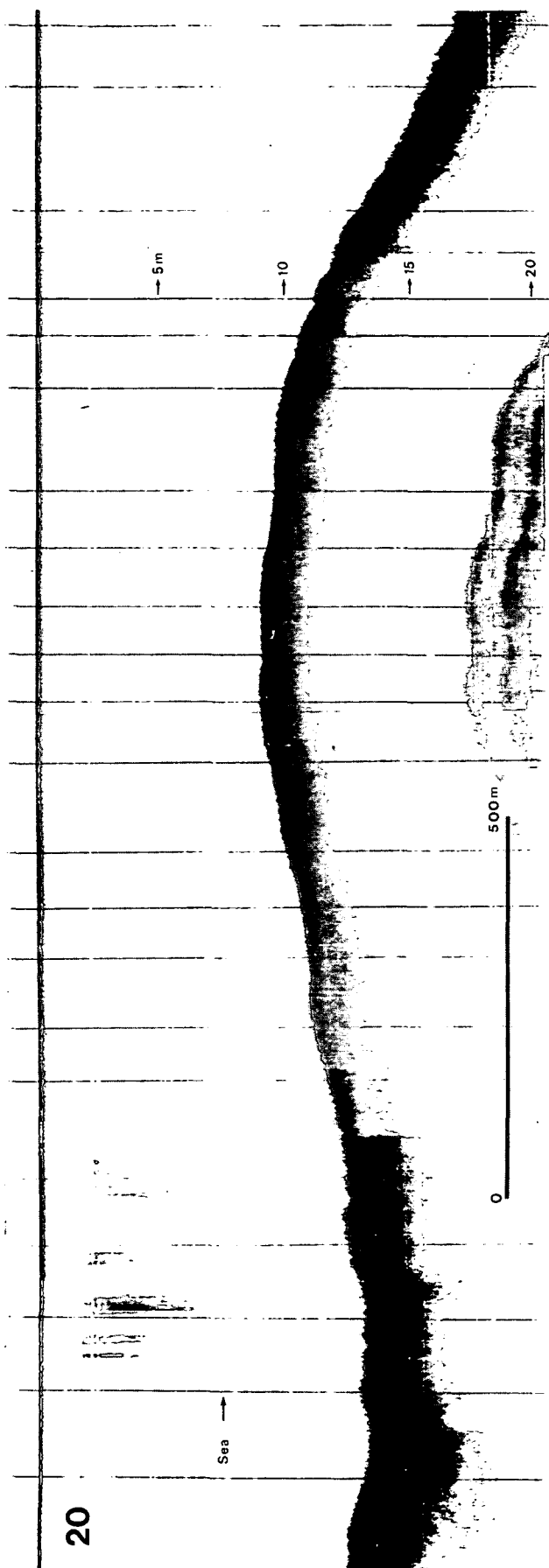
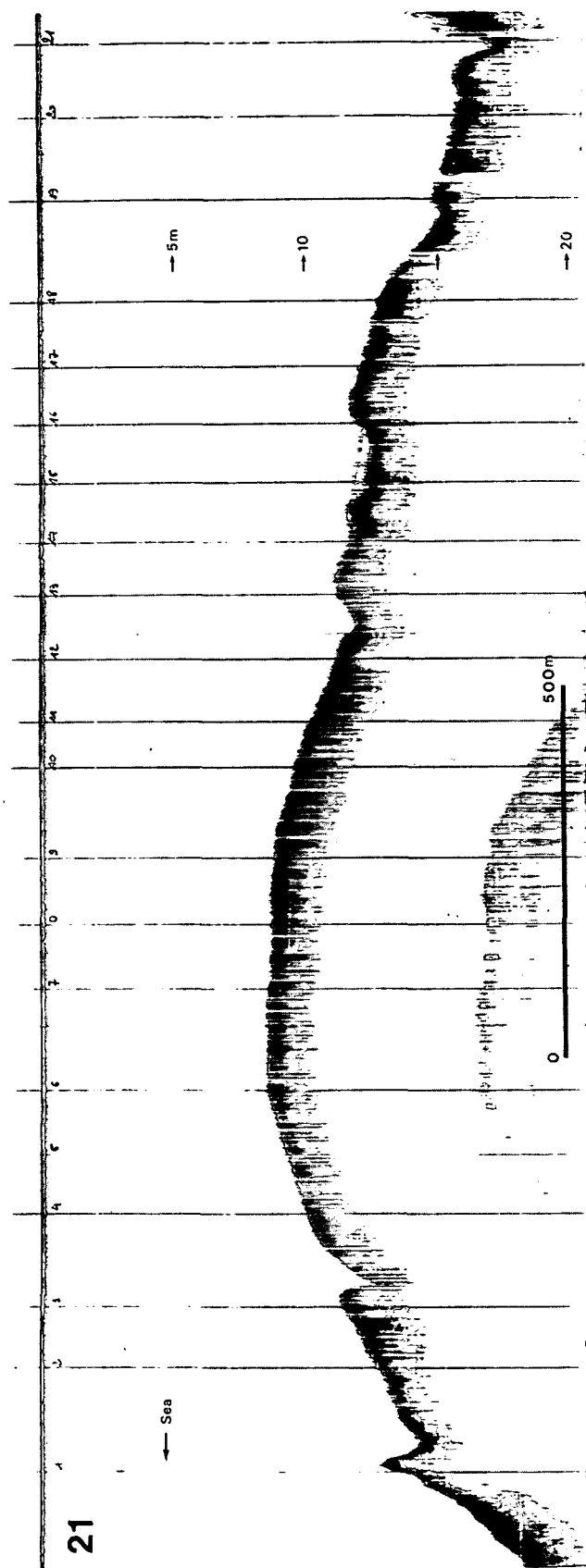


Fig. 10 Bottom profiles 20 and 21.

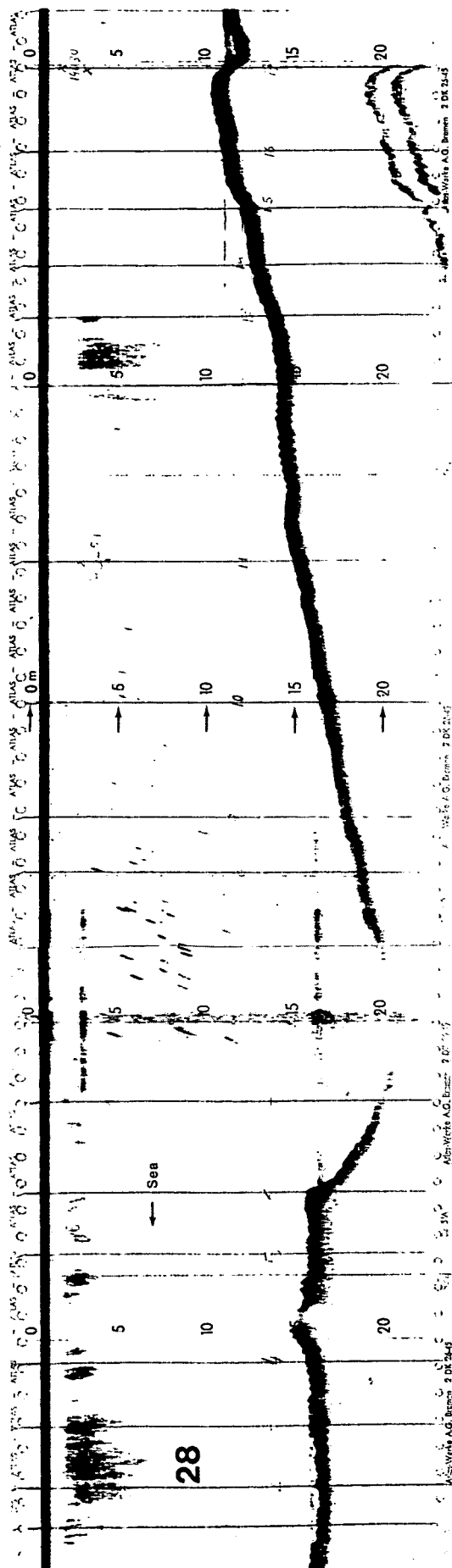


Fig. 11 Bottom profiles 22 and 28.

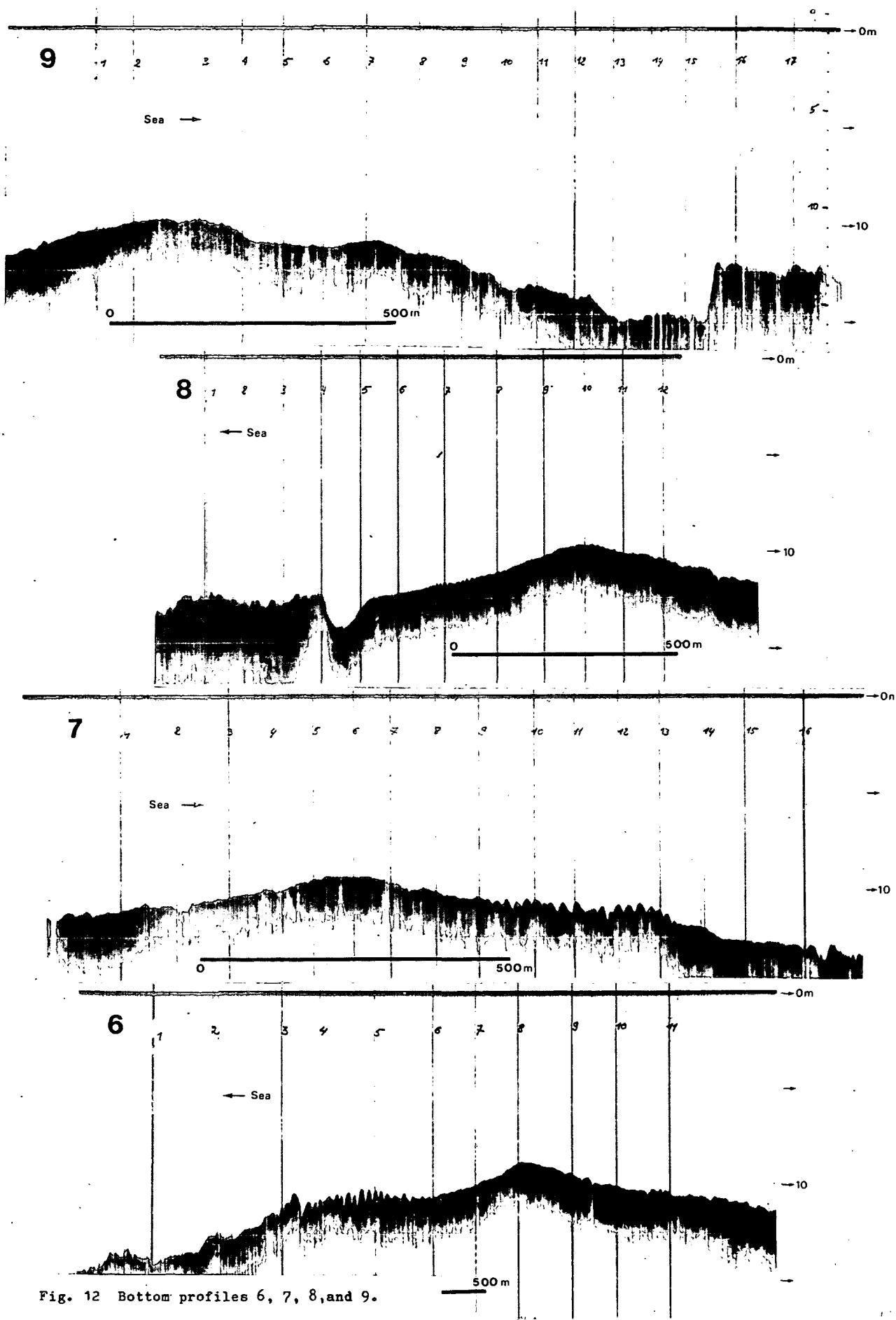


Fig. 12 Bottom profiles 6, 7, 8, and 9.

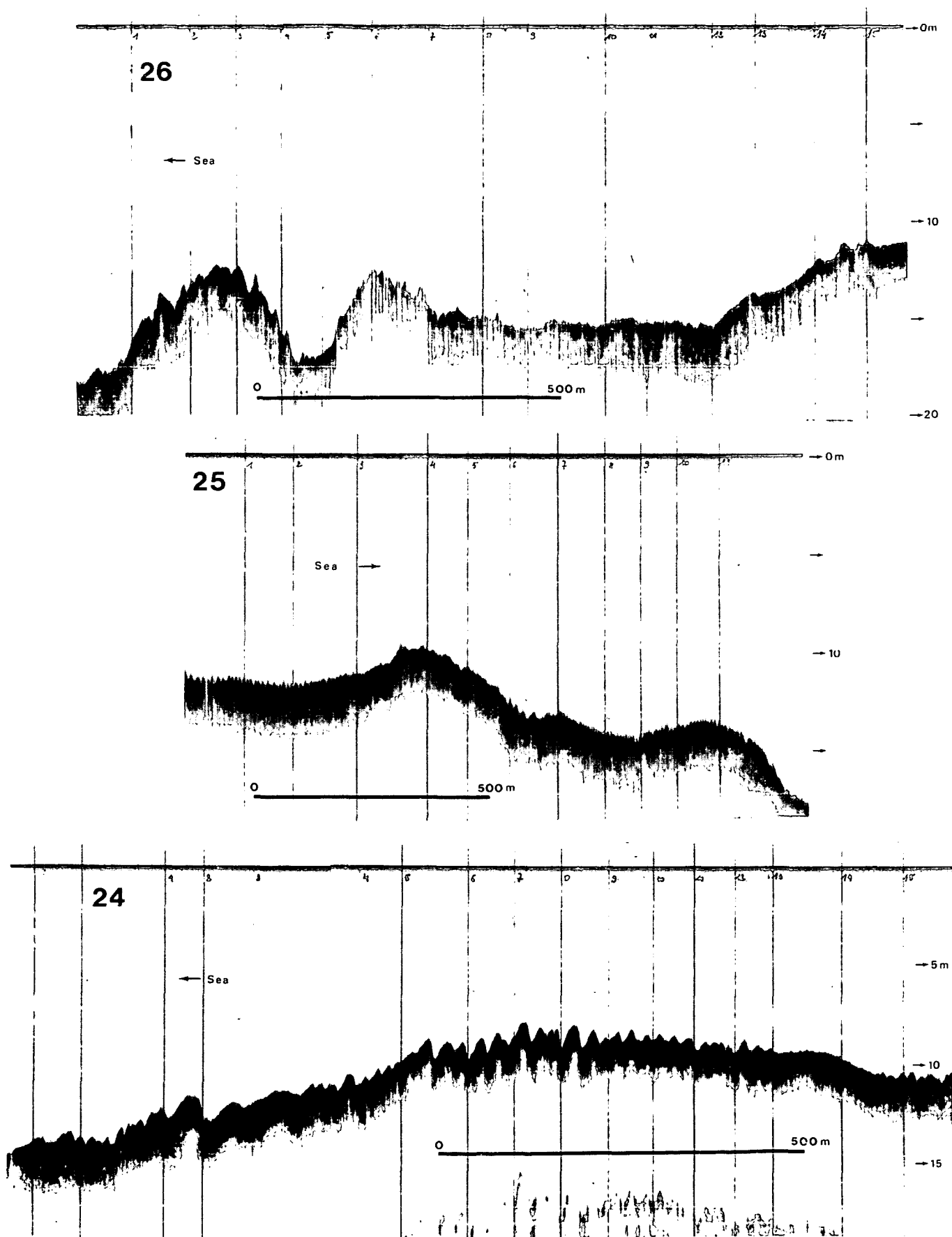


Fig. 13 Bottom profiles 24, 25 and 26.

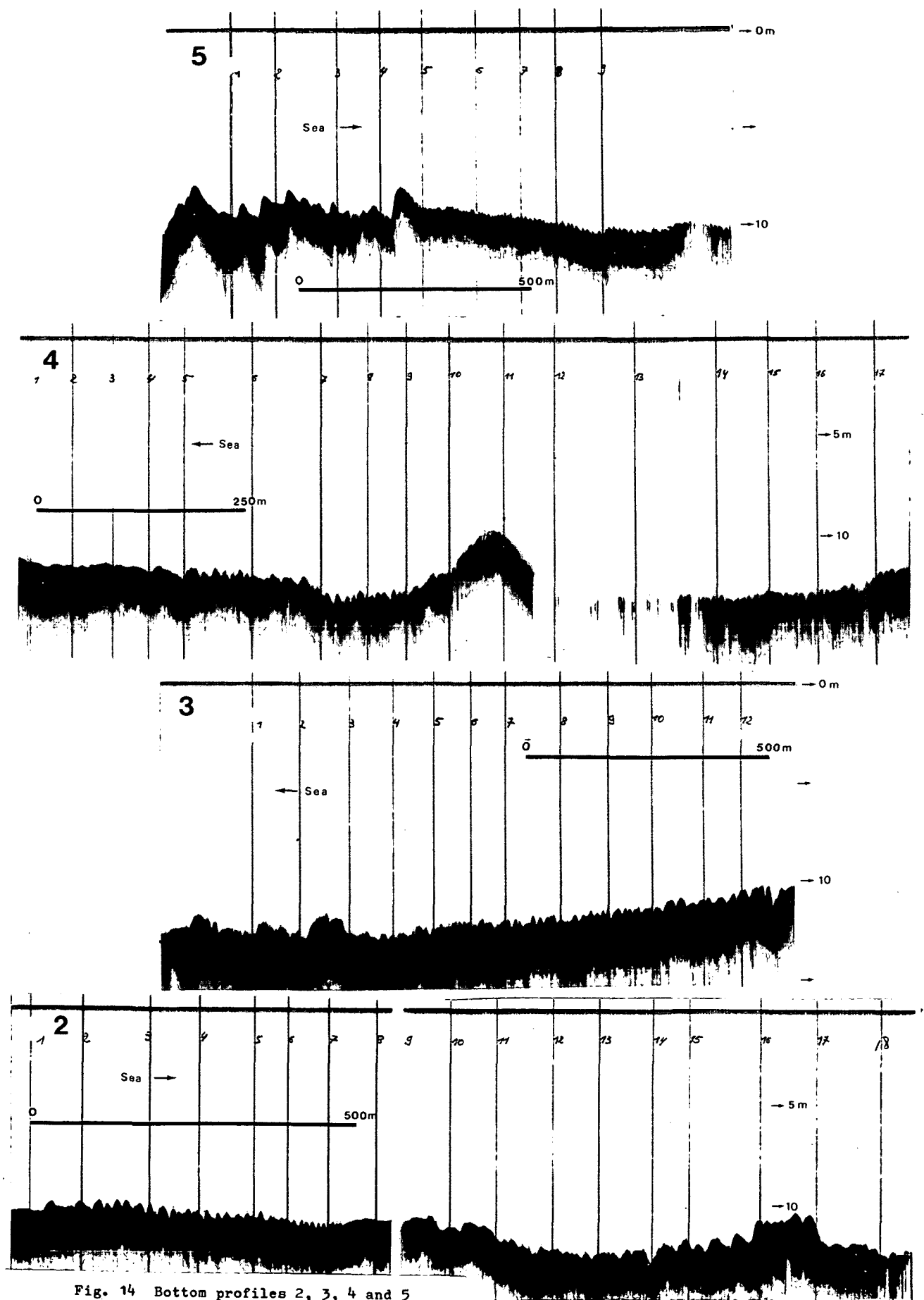


Fig. 14 Bottom profiles 2, 3, 4 and 5

